## Quantum controlled cluster states in an optical parametric oscillator with a structured light pump

R. F. Barros, <sup>1</sup> G. B. Alves, <sup>1</sup> O. Pfister, <sup>2</sup> and A. Z. Khoury <sup>1</sup>

<sup>1</sup>Instituto de Física, Universidade Federal Fluminense, CEP 24210-346, Niterói-RJ, Brazil\*

<sup>2</sup>Department of Physics, University of Virginia, Charlottesville, Virginia 22903, USA

We investigate the multipartite entanglement between spatial and spectral modes of an optical parametric oscillator pumped with a structured light field. When the pump beam is prepared in a second-order transverse mode, we show that the down-converted signal and idler fields are generated in a reconfigurable quadripartite entangled state of first-order modes. Our investigation is based both on separability criteria and a thorough analysis of the squeezing properties. Additionally, we demonstrate that large-scale entangled states can be produced and easily controlled by a pump field structured in both spatial and spectral domains. Our results pave the way for versatile cluster state engineering with structured light modes.

Introduction.—Practical quantum optical computers have become closer to reality after recent developments with optical parametric oscillators (OPO). The OPO is a versatile device capable of generating large-scale entanglement in either time, frequency, or spatial domains. In the time domain, for example, a scheme with multiple degenerate OPOs and staggered Einstein-Podolsky-Rosen (EPR) pairs was shown to produce cluster states with up to  $\sim 10^6$  entangled modes, with a few available at a time [1, 2]. More recently, the same approach was used to generate a square lattice cluster state, a universal resource for one-way quantum computing [3].

An alternative approach uses a spectrally shaped pump beam to tailor the interaction between the frequency modes of a single non-degenerate OPO – also known as a quantum optical frequency comb (QOFC). Such device was shown to produce different outcomes, be it in the form of parallel copies of low-dimensional states [4] or large-scale cluster states [5, 6]. More recently, a novel scheme was proposed to produce square lattice cluster states via phase-modulation of the QOFC [7], which is promising for integrated quantum photonics. Nonetheless, a singular technique of synchronously pumping the OPO with a pulsed laser was also proven to produce cluster states [8, 9], with modes encoded in the temporal shape of the downconverted fields.

On a lower scale, the spatial degree of freedom was also shown to improve the capabilities of currently available systems by increasing the dimensionality of the parameter space. For example, one could mention the production of multipartite entanglement between first-order spatial modes in a type-II OPO [10–13]. In a series of recent reports, several cluster states have also been produced with orbital angular momentum (OAM) modes in a four-wave mixing setup [14–19], with applications to quantum teleportation and quantum networks. One should also mention the proposals for production of both spatial-only [20] and spatiotemporal [21] (spatial plus frequency) graph states with OAM modes in the OPO.

In this letter, we show that an OPO pumped with

structured light fields can generate reconfigurable cluster states in the spatial domain. We show that the concurrent nonlinear interactions arising from the spatial selection rules can be easily manipulated with the pump spatial structure, leading to outcomes only obtained so far with phase-matching engineering. We also demonstrate that a spatio-spectrally shaped pump produces easily tunable large-scale cluster states in the QOFC of a single OPO. Such degree of quantum control may find different uses in quantum information, including but not limited to measurement-based quantum computing and quantum networks.

Formalism.—The linearized Hamiltonian of the optical parametric interaction is the following [22]

$$\hat{H} = i\hbar\kappa \sum_{mn} G_{mn} \hat{a}_m^{\dagger} \hat{a}_n^{\dagger} - G_{mn}^* \hat{a}_m \hat{a}_n , \qquad (1)$$

where  $\hat{a}_{m,n}^{\dagger}$  ( $\hat{a}_{m,n}$ ) are the creation (annihilation) operators of the downconverted modes and  $\kappa$  is a coupling strength, which is proportional to the second-order susceptibility. The matrix **G** is the adjacency matrix of the Hamiltonian graph [23, 24], which depends on the pump amplitude and on the spatial overlap between pump (p), signal (s) and idler (i) transverse modes. In the case of perfect phase-matching, it can be generally written as

$$G_{mn} = \sum_{l} \alpha_{l} \Lambda_{lmn} , \qquad (2)$$

where  $\alpha_l$  is the complex amplitude of the pump mode l. The intermode coupling is given by the transverse overlap integral  $\Lambda_{lmn} = \int d^2r \, u_l^{(p)}(\mathbf{r}) u_m^{(s)*}(\mathbf{r}) u_n^{(i)*}(\mathbf{r})$  [25, 26], which contains the spatial selection rules of the interaction.

The evolution of the vacuum states under the Gaussian Hamiltonian (1) can be cast within the symplectic formalism in a simple way [24, 27]. We first define the vector  $\hat{\mathbf{x}} = (\hat{q}_1 \dots \hat{q}_j \dots \hat{q}_N \ \hat{p}_1 \dots \hat{p}_j \dots \hat{p}_N)^T$ , where N is the number of interacting modes, with the field quadratures given by  $\hat{q}_j = \hat{a}_j + \hat{a}_j^{\dagger}$  and  $\hat{p}_j = -i(\hat{a}_j - \hat{a}_j^{\dagger})$ . The Heisenberg evolution of the field quadratures then takes the

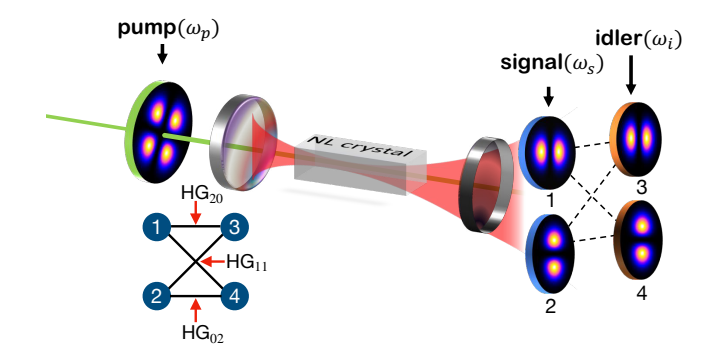


Figure 1. Illustration of the OPO with a second-order structured light pump with frequency  $\omega_0$  producing signal and idler with frequencies  $\omega_s$  and  $\omega_i$ , respectively, both in first-order Hermite-Gaussian spatial modes. The inset shows the spatial modes of the pump responsible for each pairwise interaction.

simple form  $\hat{\mathbf{x}}(t) = \mathbf{S} \hat{\mathbf{x}}(0)$ , where **S** is a symplectic matrix given by  $\mathbf{S} = e^{\gamma \mathbf{M}}$ , with

$$\mathbf{M} = \begin{pmatrix} \operatorname{Re}(\mathbf{G}) & \operatorname{Im}(\mathbf{G}) \\ \operatorname{Im}(\mathbf{G}) & -\operatorname{Re}(\mathbf{G}) \end{pmatrix}, \tag{3}$$

and  $\gamma = 2\kappa t$  for an interaction time t. Assuming a vacuum input, for which  $\mathbf{V}(0) = \mathbf{I}$  (identity matrix), the covariance matrix after the interaction can be easily obtained from (3) as  $\mathbf{V}(t) = \mathbf{S}\mathbf{S}^T$  [24]. The covariance matrix contains the full information on the output Gaussian state, which allows us to directly apply separability criteria to study the multimode entanglement properties.

Our goal is to investigate the manipulation of the multipartite entanglement using the pump spatial structure. As a first example, we consider the case of a second order pump mode, whose electric field can be generally written in the Hermite-Gaussian basis ( $HG_{mn}$ ) [28] as  $E_p = \alpha_{20}HG_{20} + \alpha_{11}HG_{11} + \alpha_{02}HG_{02}$ . As illustrated in Fig.1, such pump is optimally coupled to downconverted fields in the modes  $HG_{10}$  and  $HG_{01}$ . For each pair of signal and idler frequencies, we can name the modes as  $\{\hat{a}_1, \hat{a}_2, \hat{a}_3, \hat{a}_4\} = \{\hat{a}_{10}^{(s)}, \hat{a}_{01}^{(s)}, \hat{a}_{10}^{(i)}, \hat{a}_{01}^{(i)}\}$ , where s and s stand for signal and idler, respectively, so that  $\mathbf{G}$  can be written as

$$\mathbf{G} = \begin{pmatrix} \mathbf{0} & \alpha \\ \alpha & \mathbf{0} \end{pmatrix} \,, \tag{4}$$

$$\boldsymbol{\alpha} = \begin{pmatrix} \alpha_{20} & \alpha_{11} \frac{\sqrt{2}}{2} \\ \alpha_{11} \frac{\sqrt{2}}{2} & \alpha_{02} \end{pmatrix} , \tag{5}$$

up to a multiplicative constant that can be absorbed into the squeezing parameter  $\kappa$ .

Multipartite entanglement.—The entanglement can be analyzed by means of the positivity under partial transposition. We calculate the smallest symplectic eigenvalues of the partially transposed covariance matrix (PPT value), and apply the Peres-Horodecki separability criterion (PPT criterion) [29, 30] to all seven bipartitions,

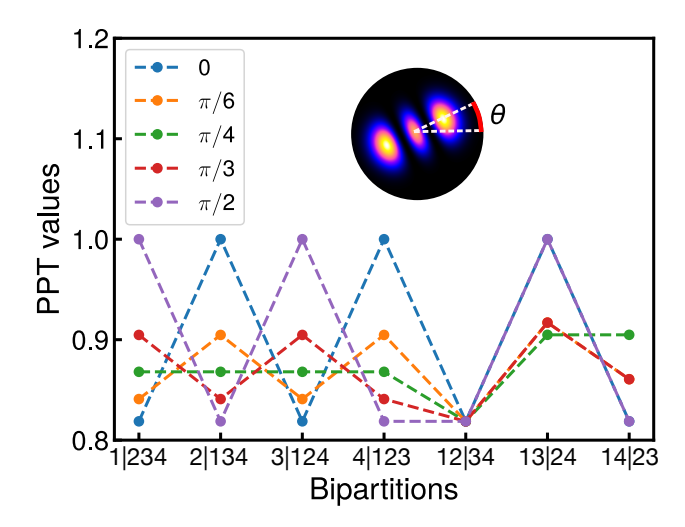


Figure 2. PPT values for a  $HG_{20}$  pump rotated by an angle  $\theta$  counterclockwise, and  $\gamma = 0.1$ . The inset illustrates the spatial profile of the pump intensity and the multiple curves are for different values of  $\theta$ .

namely (1) 1|234, (2) 2|134, (3) 3|124, (4) 4|123, (5) 12|34, (6) 13|24 and (7) 14|23. With our definitions, a PPT value lower than unit is sufficient to witness entanglement in the corresponding bipartition. We show in Fig.2 the PPT values for  $\alpha_{20} = \cos^2 \theta$ ,  $\alpha_{02} = \sin^2 \theta$  and  $\alpha_{11} = -(\sin 2\theta)/\sqrt{2}$ , which represents a HG<sub>20</sub> mode rotated by  $\theta$  counterclockwise.

Notice that genuine quadripartite entanglement exists for any  $\theta$  between 0 and  $\pi/2$ , in which case all three Hermite-Gaussian components of the pump are present. In the extreme case of  $\theta=0$  ( $\theta=\pi/2$ ), the pump only couples the modes 1 and 3 (2 and 4), breaking the quadripartite entanglement in the system. In all cases, the PPT value of partition 5 remains unaffected, which is due to the fact that there will always be modes of the signal entangled with those of the idler. This result evidences the reconfigurable entanglement between spatial modes obtained by means of a rotation in the pump shape, a transformation that can be easily performed experimentally.

Another important subset of the 2nd order subspace corresponds to the combinations of Laguerre-Gaussian (LG) modes containing opposite orbital angular momenta. Such modes can be parametrized according to  $\alpha_{11} = \sin(\theta/2)e^{i\phi}$  and  $\alpha_{20} = -\alpha_{02} = \cos(\theta/2)/\sqrt{2}$ , where  $0 \le \theta \le \pi$  and  $0 \le \phi \le 2\pi$  are angles in the second-order orbital Poincaré sphere (PS) [31]. The LG modes with OAM  $\pm 2$  are found at  $\{\theta,\phi\} = \{\pi/2,\pi(1\mp 1/2)\}$ , while petal modes with no OAM are found at  $\{\theta,0\}$  and  $\{\theta,\pi\}$  [32]. We show in Fig. 3 the PPT values for different paths in the second-order PS.

We observe that the symplectic eigenvalues for pump modes with zero OAM only differ for the bipartitions 6 and 7. On the other hand, tuning the pump OAM with

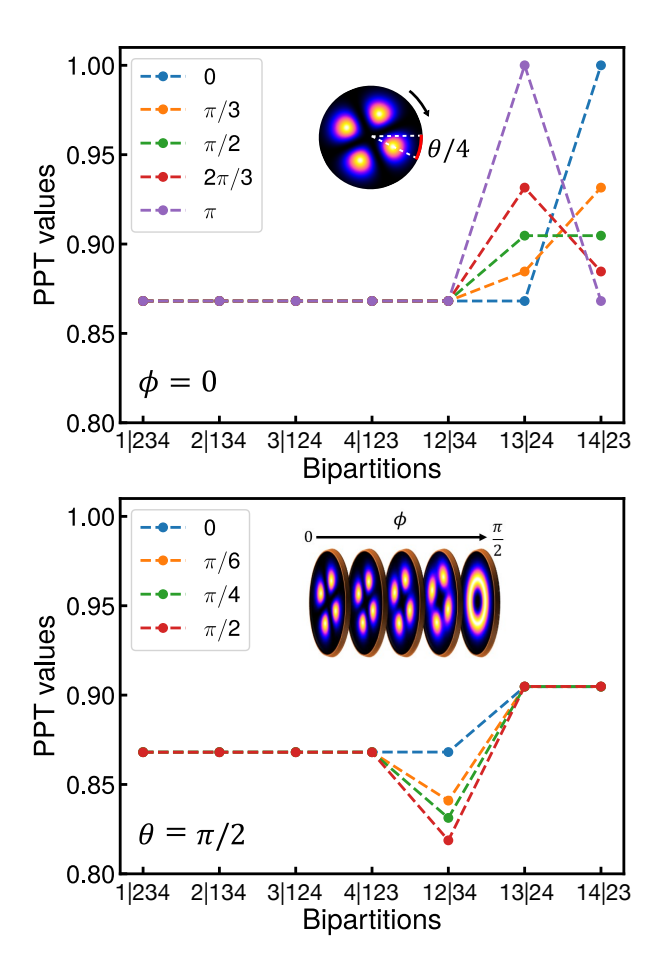


Figure 3. PPT values for a pump modes along two paths on the second-order PS:  $\phi=0$  and a variable  $\theta$  (top) and  $\theta=\pi/2$  and a variable  $\phi$  (bottom). The insets in each panel illustrate the varying spatial profile of the pump intensity for the corresponding paths. The parameters considered are such that  $\gamma=0.1$ .

the angle  $\phi$  only changes the PPT value of the bipartition 5, which is minimal for  $\phi=\pi(1\pm1/2)$ , reaching the same value as in Fig.2. This boost in the symplectic eigenvalues occurs when, for some choice of measurement basis, the downconverted fields are constrained to a single pair of transverse modes. In the case of Fig.2, for example, a rotated HG<sub>20</sub> is optimally coupled to signal and idler in a HG<sub>10</sub> mode rotated by the same angle. The same occurs for the pump carrying OAM  $\pm 2$ , which produces two identical downconverted modes with OAM  $\pm 1$ , due to the OAM conservation in the parametric process. Therefore, there is a compromise between the amount of entanglement, as measured by the minimum symplectic eigenvalue, and the multipartite distribution of entanglement.

To further analyze the entanglement structure of the downconverted fields, we study the eigenmode decomposition of the matrix (3). The combinations of quadratures that diagonalize  $\mathbf{M}$ , also called supermodes [22,33],

are squeezed (anti-squeezed) when corresponding to negative (positive) eigenvalues. The analysis for an arbitrary pump is somewhat involved, but it becomes simpler for modes in the PS. In this case, the two negative eigenvalues, are given by

$$\lambda_{\pm}^{(S)} = -\gamma \sqrt{\frac{1 \pm \sin \theta \sin \phi}{2}}, \qquad (6)$$

with the positive eigenvalues given by  $\lambda_{\pm}^{(AS)} = -\lambda_{\pm}^{(S)}$ . There are eight supermodes, so each eigenvalue is two-fold degenerate. For the case of the bottom panel of Fig.3  $(\theta=\pi/2 \text{ and variable } \phi)$ , for example, we see that the  $\lambda_{\pm}^{(S)}$  is maximized for a pump with OAM  $\pm 2$ , in which case  $\lambda_{\mp}^{(S)}$  vanishes. This is consistent with the result of Fig.3, in the sense that a higher squeezing level leads to stronger entanglement, suggested, in this case, by the stronger violation of the PPT criterion. On the other hand, for a pump in the rotating petal mode shown in the top panel of Fig. 3  $(\phi=0 \text{ and variable } \theta)$ , we have  $\lambda_{\pm}^{(S)} = -\gamma/\sqrt{2}$  for all  $\theta$ , also consistent with the opposing variation of the PPT values of the bipartitions 6 and 7, with all others kept fixed.

The supermodes for an arbitrary pump in the secondorder PS are combinations of the  $\hat{p}'s$  and  $\hat{q}'s$  of the four downconverted modes, which are more easily identified in terms of the first order Laguerre-Gaussian (LG) [28] basis operators  $\hat{a}_{\pm}^{(s)} = (\hat{a}_1 \mp i\hat{a}_2)/\sqrt{2}$  and  $\hat{a}_{\pm}^{(i)} = (\hat{a}_3 \mp i\hat{a}_4)/\sqrt{2}$ . In this basis, the pump phases can be absorbed by a suitable redefinition of the field operators, leading to EPR-like correlations between generalized quadratures rotated in phase space [34].

Spatio-spectral cluster states.—Now we discuss how a structured pump can be used to generate large-scale entanglement in the quantum optical frequency comb (QOFC) of a single OPO [4–6]. A QOFC is usually obtained from a type-I OPO operating below threshold and close to degeneracy, which features several longitudinal modes simultaneously close to resonance [35, 36]. The downconverted frequencies are  $\omega_n = \omega_0 + n\delta$ , where  $\omega_0$  is an arbitrary offset and  $\delta$  is the cavity free spectral range. Due to energy conservation, the pair  $\{n_1, n_2\}$  only couples to a pump frequency given by  $\omega_p = 2\omega_0 + p\delta$ , where  $p = n_1 + n_2$  is the pump index. Therefore, each spectral component p of the pump produces multiple EPR pairs dispersed in the frequency domain.

In this context, pumping the OPO with a monochromatic field carrying a second-order spatial mode yields the parallel production of several copies of the quadripartite entangled state described previously. The number of copies is only limited by the phase-matching bandwidth, which usually encompasses  $\sim 10^4$  modes. Also importantly, for pump structures in the second-order PS, one can show that the adjacency matrix  $\bf G$  is self-inverse ( $\bf G^2 = \bf I$ ), meaning that a multipartite state produced by this method is an arbitrarily good approximation to

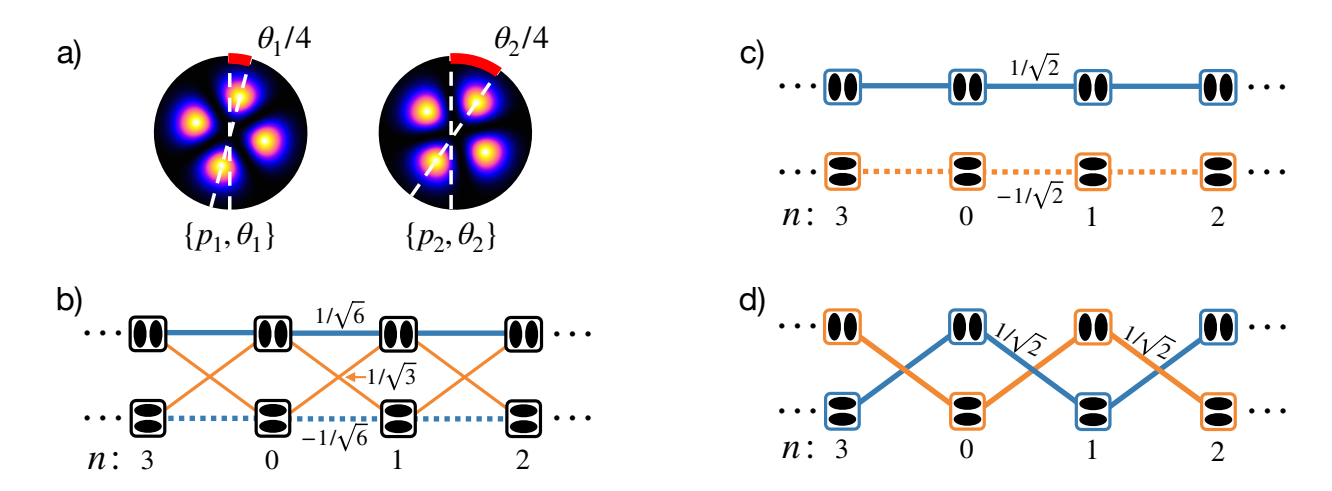


Figure 4. Cluster states produced by dual-frequency spatially structured pump with  $A_1 = A_2 = 1/\sqrt{2}$ . In (a) we show the considered pump modes, with petal shapes carrying no OAM. The produced cluster states are shown for  $p_1 = 1$  and  $p_2 = 3$ , and the following combinations of spatial modes: (b)  $\theta_1 = \theta_2 = \pi/2$ , (c)  $\theta_1 = \theta_2 = 0$  and (d)  $\theta_1 = \theta_2 = \pi$ . While in (b) the cluster has a dual-rail structure, in (c) and (d) it is dismantled in two independent single-rail clusters. The numbers in (b), (c) and (d) are the weights of the cluster edges.

a canonical cluster state of graph G, after Fourier transforms ( $\pi/2$  phase shifts) on either the signal or idler modes [23].

Without a spatially structured pump, an equivalent outcome has only been obtained using the pump polarization and crystal engineeging to phase match three concurrent nonlinearities [4]. With spatial modes, the concurrent nonlinear processes are uncorrelated to the wavevector mismatch, which eliminates the need for special crystal designs. Besides, the number of concurrent processes with spatial modes increases with the pump order, which suggests the possibility of parallel generation of multipartite entangled states of higher dimensions.

To further highlight the advantages of using spatial modes for the production of CV multipartite entanglement, we also consider a dual-frequency pump whose spectral components  $p_1$  and  $p_2$  obey  $|p_1-p_2|=2$ . This is a well stablished technique to generate large-scale cluster states in the QOFC, as detailed in Ref.[5]. We write the pump field as  $E_p = A_1 E(\alpha_1, p_1) + A_2 E(\alpha_2, p_2)$ , where  $\alpha_j$  refers to Eq.(5) and  $A_j$  are constant amplitudes. The corresponding Hamiltonian is given by

$$\hat{H} = i\kappa' \hbar \sum_{n} \left( V_n^T \bar{\mathbf{G}} V_n - H.C \right) , \qquad (7)$$

where the summation is over the frequencies of the QOFC, and

$$\bar{\mathbf{G}} = \begin{pmatrix} \mathbf{0} & A_{1} \boldsymbol{\alpha}_{1} & \mathbf{0} \\ A_{1} \boldsymbol{\alpha}_{1} & \mathbf{0} & A_{2} \boldsymbol{\alpha}_{2} \\ \mathbf{0} & A_{2} \boldsymbol{\alpha}_{2} & \mathbf{0} \end{pmatrix}, V_{n} = \begin{pmatrix} \hat{b}_{p_{1}-n}^{\dagger} \\ \hat{c}_{p_{1}-n}^{\dagger} \\ \hat{b}_{n}^{\dagger} \\ \hat{c}_{n}^{\dagger} \\ \hat{b}_{p_{2}-n}^{\dagger} \\ \hat{c}_{p_{2}-n}^{\dagger} \end{pmatrix}. \tag{8}$$

In the above equation,  $\kappa' = \kappa/2$  and we have renamed the operators  $\hat{a}_{10}^j$  and  $\hat{a}_{01}^j$  as  $\hat{b}_j$  and  $\hat{c}_j$ , respectively, where j is the frequency index.

For simplicity, we consider that the spatial modes of the two pumps are second-order petals, as shown in Fig.4a, such that  $\alpha_j = \alpha_j(\theta_j, \phi_j = 0)$  and the total pump field becomes  $E_p = A_1 E(p_1, \theta_1) + A_2 E(p_2, \theta_2)$ . In this case, one can show that the squeezed supermodes obtained from (7) are the nullifiers of a cluster state known as a dual-rail quantum wire [1, 5], shown in Fig.4b. In addition, for certain angles of the pump petals the dual-rail structure can be dismantled in two independent single-rail clusters, as shown in Figs.4c and 4d. This particular example is already sufficient to show that pumping an OPO with structured light provides an efficient way to implement quantum control on the QOFC.

Conclusion.—We have investigated the multipartite entanglement resulting from an OPO with a pump beam structured in the hybrid spatial-spectral domain. Considering different second-order spatial modes in a monochromatic pump, we have shown that a reconfigurable quadripartite state can be achieved by a simple rotation of the pump profile. We have also demonstrated that a dualfrequency pump in a combination of second-order spatial modes yields large-scale cluster states in the spatially structured frequency comb. In both cases, we show that changing the pump spatial structure alone is sufficient to tailor the multimode interaction, thereby allowing the easy quantum control of the produced states. Our results pave the way for the versatile production of cluster states in the QOFC, with potential applications to measurement-based quantum computing.

Acknowledgements.—This work was supported by Coordenação de Aperfeiçoamento de Pessoal de Nível Superior

(CAPES), Fundação Carlos Chagas Filho de Amparo à Pesquisa do Estado do Rio de Janeiro (FAPERJ), Instituto Nacional de Ciência e Tecnologia de Informação Quântica (INCT-IQ) and Conselho Nacional de Desenvolvimento Científico e Tecnológico (CNPq). O.P. was supported by NSF grant PHY-1820882.

- \* rafael.fprb@gmail.com
- S. Yokoyama, R. Ukai, S. C. Armstrong, C. Sornphiphatphong, T. Kaji, S. Suzuki, J.-i. Yoshikawa, H. Yonezawa, N. C. Menicucci, and A. Furusawa, Nature Photonics 7, 982 (2013).
- [2] J.-i. Yoshikawa, S. Yokoyama, T. Kaji, C. Sorn-phiphatphong, Y. Shiozawa, K. Makino, and A. Furusawa, APL Photonics 1, 060801 (2016), https://doi.org/10.1063/1.4962732.
- [3] W. Asavanant, Y. Shiozawa, S. Yokoyama, B. Charoensombutamon, H. Emura, R. N. Alexander, S. Takeda, J.i. Yoshikawa, N. C. Menicucci, H. Yonezawa, and A. Furusawa, Science 366, 373 (2019).
- [4] M. Pysher, Y. Miwa, R. Shahrokhshahi, R. Bloomer, and O. Pfister, Phys. Rev. Lett. 107, 030505 (2011).
- [5] M. Chen, N. C. Menicucci, and O. Pfister, Phys. Rev. Lett. 112, 120505 (2014).
- [6] N. C. Menicucci, S. T. Flammia, and O. Pfister, Phys. Rev. Lett. 101, 130501 (2008).
- [7] X. Zhu, C.-H. Chang, C. González-Arciniegas, A. Pe'er, J. Higgins, and O. Pfister, Hypercubic cluster states in the phase modulated quantum optical frequency comb (2020), arXiv:1912.11215 [quant-ph].
- [8] J. Roslund, R. M. de Araújo, S. Jiang, C. Fabre, and N. Treps, Nature Photonics 8, 109 (2014).
- [9] Y. Cai, J. Roslund, G. Ferrini, F. Arzani, X. Xu, C. Fabre, and N. Treps, Nature Communications 8, 15645 (2017).
- [10] B. C. dos Santos, K. Dechoum, and A. Z. Khoury, Phys. Rev. Lett. 103, 230503 (2009).
- [11] K. Liu, J. Guo, C. Cai, S. Guo, and J. Gao, Phys. Rev. Lett. 113, 170501 (2014).
- [12] K. Liu, J. Guo, C. Cai, J. Zhang, and J. Gao, Opt. Lett. 41, 5178 (2016).
- [13] C. Cai, L. Ma, J. Li, H. Guo, K. Liu, H. Sun, R. Yang, and J. Gao, Photon. Res. 6, 479 (2018).

- [14] R. Pooser and J. Jing, Phys. Rev. A 90, 043841 (2014).
- [15] X. Pan, S. Yu, Y. Zhou, K. Zhang, K. Zhang, S. Lv, S. Li, W. Wang, and J. Jing, Phys. Rev. Lett. **123**, 070506 (2019).
- [16] S. Li, X. Pan, Y. Ren, H. Liu, S. Yu, and J. Jing, Phys. Rev. Lett. 124, 083605 (2020).
- [17] K. Zhang, W. Wang, S. Liu, X. Pan, J. Du, Y. Lou, S. Yu, S. Lv, N. Treps, C. Fabre, and J. Jing, Phys. Rev. Lett. 124, 090501 (2020).
- [18] S. Liu, Y. Lou, and J. Jing, Nature Communications 11, 3875 (2020).
- [19] W. Wang, K. Zhang, and J. Jing, Phys. Rev. Lett. 125, 140501 (2020).
- [20] J. Zhang, J. J. Wang, R. G. Yang, K. Liu, and J. R. Gao, Opt. Express 25, 27172 (2017).
- [21] R. Yang, J. Zhang, I. Klich, C. González-Arciniegas, and O. Pfister, Phys. Rev. A 101, 043832 (2020).
- [22] G. Patera, C. Navarrete-Benlloch, G. J. de Valcárcel, and C. Fabre, The European Physical Journal D 66, 241 (2012).
- [23] N. C. Menicucci, S. T. Flammia, H. Zaidi, and O. Pfister, Phys. Rev. A 76, 010302 (2007).
- [24] N. C. Menicucci, S. T. Flammia, and P. van Loock, Phys. Rev. A 83, 042335 (2011).
- [25] C. Schwob, P. Cohadon, C. Fabre, M. Marte, H. Ritsch, A. Gatti, and L. Lugiato, Applied Physics B 66, 685 (1998).
- [26] G. B. Alves, R. F. Barros, D. S. Tasca, C. E. R. Souza, and A. Z. Khoury, Phys. Rev. A 98, 063825 (2018).
- [27] R. Simon, E. C. G. Sudarshan, and N. Mukunda, Phys. Rev. A 37, 3028 (1988).
- [28] A. Yariv, Optical electronics, 4th ed., HRW series in electrical engineering (Saunders College Publishing, Philadelphia, Pa.; Sydney, 1991).
- [29] A. Peres, Phys. Rev. Lett. 77, 1413 (1996).
- [30] R. Simon, Phys. Rev. Lett. 84, 2726 (2000).
- [31] M. J. Padgett and J. Courtial, Opt. Lett. 24, 430 (1999).
- [32] A. M. Yao and M. J. Padgett, Adv. Opt. Photon. 3, 161 (2011).
- [33] H. Wang, K. Zhang, N. Treps, C. Fabre, J. Zhang, and J. Jing, Phys. Rev. A 102, 022417 (2020).
- [34] G. Leuchs, R. Dong, and D. Sych, New Journal of Physics 11, 113040 (2009).
- [35] R. C. Eckardt, C. D. Nabors, W. J. Kozlovsky, and R. L. Byer, J. Opt. Soc. Am. B 8, 646 (1991).
- [36] R. F. Barros, G. B. Alves, and A. Z. Khoury, Spatially structured frequency combs in optical parametric oscillators (2020), arXiv:2010.11145 [physics.optics].